

CHARACTERIZATION AND INVESTIGATION OF HEAT TRANSFER ENHANCEMENT IN POOL BOILING WITH WATER-ZnO NANOFLUID

by

**Jagdeep M. KSHIRSAGAR, Ramakant SHRIVASTAVA*,
and Prakash S. ADWANI**

Department of Mechanical Engineering, Government Engineering College, Aurangabad, India

Original scientific paper
<https://doi.org/10.2298/TSCI150516200K>

The main focus of the present work is to characterize the ZnO nanoparticles further to prepare the ZnO nanofluid with base fluid as deionised water and to investigate enhancement in critical heat flux at different weight concentrations of nanofluids. The size of nanoparticles is found to be 55.25 nm.

To study critical heat flux enhancement using ZnO nanofluid, different weight concentration of nanofluid are prepared. It is observed that maximum enhancement is 47.16% for 1.5 wt.% of ZnO nanofluid. Surface roughness and scanning electron microscopy of heater surface is carried out for all weight concentrations of nanofluid, which shows increase in R_a value up to some extent then it decreases and porosity on the surface of heater observed in scanning electron microscopy, is the source to enhance critical heat flux.

Keywords: *nanoparticles, nanofluid, critical heat flux, deionised water, enhancement*

Introduction

Heat transfer is an important issue in many industrial applications. The heat transfer in the nucleate boiling regime, the latent heat of vaporization during the change from liquid to gas phase can be exploited and is the most effective way of cooling thermal systems operating at high temperatures [1]. However, the boiling heat transfer is restricted by the critical heat flux (CHF). This is highest heat flux where boiling heat transfer sustains its high cooling performance. When the surface reaches CHF, it becomes coated with a vapour film which isolates the heating surface and the fluid thus the heat transfer decreases drastically [1-3]. In these conditions, the wall temperature rises quickly, and if it exceeds the limits of its constituent materials, system failure occurs. For this reason, every system incorporates a safety margin by running at a heat flux lower than CHF, but this approach reduces system efficiency [1]. This compromise between safety and efficiency is a serious problem in the industry. For this reason, a huge work has been carried out to understand heat transfer mechanisms in nucleate boiling and CHF conditions and to increase the CHF.

Pioro *et al.* [4, 5] present a very fine review of the parametric effect of boiling surface and prediction methods. They show that it is complex problems involving many inter linked parameters affect heat transfer performances. Their analysis of the literature shows that some results seem contradictory. For example, some researchers conclude that for many practical

*Corresponding author, e-mail: ramakant.shrivastava@gmail.com

applications the effect of solid/liquid/vapour interaction on the heat transfer coefficient in nucleate boiling conditions can be ignored (except for the cryogenic fluid), whereas others conclude that these effects are important [4]. Some studies have firm on evaluating the effect of surface characteristics on heat transfer performance. These parameters are typically the contact angle, thermophysical properties, thickness, orientation in space, roughness (surface finish), and microstructure (shape, dimensions, pore density for the vapour bubble generating centre) [4]. All these interlinked parameters simultaneously affect heat transfer performance. At the moment, there is not sufficient information to solve this complex problem and for this reason, only separate effects are considered [4]. Enhancement in CHF also noted in the literature for all nanofluids with different orientation and heater surfaces [6].

In present case, micro-structure and wettability are the most important aspects. These parameters are dealt with in the literature, remarkably, Kim *et al.* [7] worked with Al₂O₃ and TiO₂ nanofluid. They concluded that a nanoparticle coating on a heating surface is a prime factor in enhancing the CHF of nanofluids. The main factors that explain this behaviour are wettability and capillary wicking.

Structural and microstructure of ZnO nanoparticles

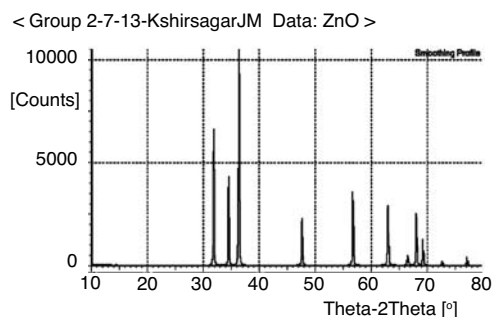


Figure 1. The XRD pattern of ZnO nanoparticle

Table 1. Properties of ZnO nanoparticles

Items	ZnO
Content of ZnO	99.9%
Average particle size	55.25 nm
Specific surface area	80 m ² /gm

results suggested the particle size less than 20 nm than more strain. Particles greater than 50 nm have less strain.

The graph shown in fig. 1 depicts that the X-ray diffraction spectra has highest intensity of 9177 counts at 36.39°. It is also observed that all Zn nanoparticles remained in pure Zn state. The scanning electron microscopy (SEM) photograph of nanopowder is shown in fig. 3.

Preparation of nanofluid and characterization

The ZnO nanoparticles were dispersed in deionized (DI) water for 12 hours under high speed mechanical stirrer (Toshiba, India). No surfactant or stabilizer were used during the preparation of nanofluid as they have some influence on forced convective heat transfer coefficient

The structural and microstructure properties of the ZnO nanoparticles are shown in fig. 1. X-ray diffraction (XRD) patterns of ZnO particles can be used to determine the size of the nanoparticles.

Structure analysis ZnO of nanoparticles

Figure 1 shows the XRD pattern of ZnO nanoparticles. All the peaks in diffraction pattern show monoclinic structure of ZnO. Average grain size calculated by using Debay-Scherrer formula is approximately 55.25 nm:

$$D = \frac{0.9\lambda}{\beta \cos \theta} \quad (1)$$

where β is the full width at half maxima of the peak in XRD pattern, θ – the angle of the peak, and λ – the wavelength of X-rays. Elastic strain is also calculated from XRD results. The strain

and overall heat transfer coefficient. After 24 hour no sedimentation of nanoparticles was found. Generally, the properties of the nanofluid depend on the properties of nanoparticles and the surface molecules taking part in the heat transfer procedure depend on the size and shape of the particles themselves, and affected by the agglomeration of the particles. As shown in fig. 2 taken by transmission electron microscopy (TEM), the particle size has a normal distribution in a range from 50 nm to 55 nm.

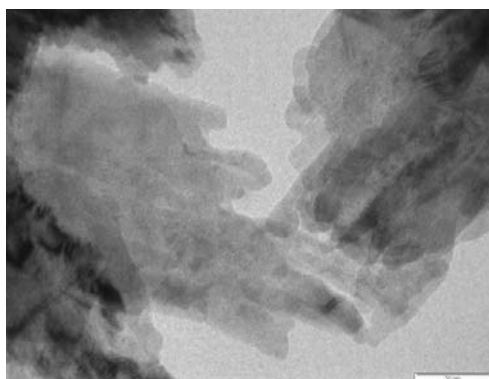


Figure 2. The TEM image of ZnO particles

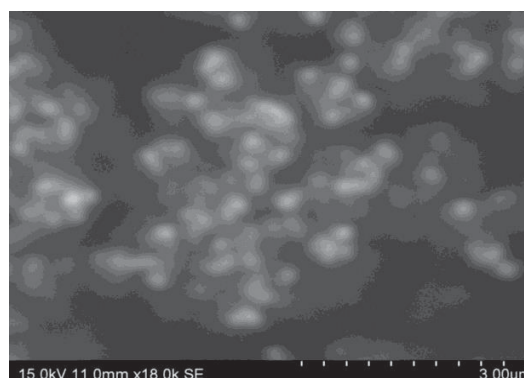


Figure 3. The SEM image of ZnO particles

Determination of enhancement in CHF

The Ni-Cr wire having 0.321 mm diameter is used as heater surface. The length of the heater is 110 mm. For benchmarking the experiment the Zuber's correlation is used initially for DI water, average CHF for ten experiments is found to 1.2 MW/m².

Theoretical determination of CHF

A number of experiments on bare Ni-Cr wires of 0.321 mm in diameter are carried out to examine the reproducibility of the experimental apparatus and get insights about the fundamental mechanism of the CHF phenomenon on the thin wire used in this study. The CHF values of pure water on bare wires showed good repeatability.

Methodology and correlation

The well known Zuber's correlation is used for validation of the test set up. Experimental values of q''_{CHF} is compared with that as predicted by Zuber's correlation:

$$q''_{CHF} = \frac{\pi}{24} \rho_g^{0.5} h_{fg} [\sigma g (\rho_l - \rho_v)]^{0.25} \quad (2)$$

But, it is known that the effect of cylinder radius on the CHF for wires is significant [8-12]. *You et al.* [12] reported in their photographic studies that the CHF on small wires were two different mechanisms which proceed to film boiling: hydrodynamic CHF and local dry out in which power is transferred from a heated surface to deionized water it is desired to obtain high heat fluxes with low temperature difference, there is linear relationship between heat fluxes and temperature difference. If heat fluxes are increased bubbles nucleate at hot surface of heater wire and depart to the sub cooled fluid and collapse. If the heat flux more increased at some point a vapour film is formed on the surface of heater. The heat transfer rate suddenly decreased and wall temperature increased the value at which it occurs is called CHF.

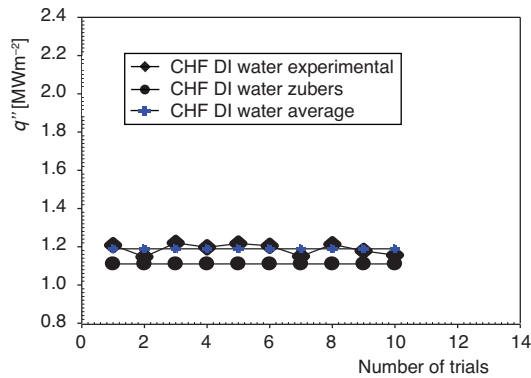


Figure 4. CHF curve experimental and theoretical Zuber's correlation of DI water

electrodes connected with the clamps in addition to this uncertainty also associated with length and diameter of the Ni-Cr wire heater [13].

In this study, the uncertainties of the measured parameters were analysed by the error propagation method. For example, uncertainty of the heat flux was calculated: heat flux is calculated using eq. (3). Thus the main source of heat flux uncertainty is found as voltage, V , current, I , diameter of heater, D , and length, L . Heat flux uncertainty can be calculated using the following equation:

$$\frac{\Delta(q)}{(q)} = \sqrt{\left(\frac{\Delta V}{V}\right)^2 + \left(\frac{\Delta I}{I}\right)^2 + \left(\frac{\Delta D}{D}\right)^2 + \left(\frac{\Delta L}{L}\right)^2} \quad (4)$$

The elemental percentage uncertainty of V , I , D , and L is less than 1.63%, 3.49%, 0.31%, and 1.81%, respectively. Thus:

$$\frac{\Delta q}{q} = \sqrt{1.63^2 + 3.49^2 + 0.31^2 + 1.81^2} \quad (5)$$

$$\frac{\Delta q}{q} = 4.26\% \quad (6)$$

Therefore, the measurement uncertainty on the calculated heat flux is $< \pm 4.26\%$. For other parameters, a similar approach was used for calculating the measurement uncertainty.

Experimental set-up

Figure 5 shows a schematic illustration of the experimental set-up. The test facility consists of Borosil glass vessel of capacity 3 litres. The glass vessel is transparent to observe the actual phenomenon of bubble formation. On top of the vessel 16 mm thickness Bakelite sheet is used to cover test vessel. Rubber gasket is used for the perfect alignment on test vessel. On sheet two holes of 5 mm diameter each, are drilled at a distance of 55 mm from centre, *i. e.* the distance between two holes are 110 mm. These holes are used for inserting and holding Cu electrodes. One hole of 20 mm diameter is drilled at the centre of the sheet to hold the condenser inlet, which collects the vapours generated in the test cell. The condenser is placed at the top of

During the experimentation, condition at breaking of wire due to CHF is noted and corresponding voltage and current are recorded. The CHF is calculated by following formula:

$$q'' = \frac{V \times I}{\pi DL} \quad (3)$$

Validation of experimental set is done for ten trials, result of that is shown in fig. 4.

Uncertainty in CHF

The main source of uncertainty of the applied voltage and current only due to contact resistance between the wire heater and

test cell. One 5 mm hole is drilled to accommodate K-type thermocouple is inserted in the test cell to measure the bulk temperature of the fluid during experimentation. An arrangement is done to hold the pre heater in the test cell on Bakelite sheet. This pre heater is used to heat bulk fluid in the test cell to saturation temperature. Vent is provided on the Bakelite sheet, so that atmospheric pressure always acts on the test cell. Two Cu electrodes of size 5 mm (diameter) \times 150 mm (length) are used for holding the test heater. The Ni-Cr wire of 28 gauge *i. e.* 0.321 mm diameter is used as heater surface. The length of the heater is 110 mm. The DC power supply with a capacity (230 V, 30 A) is used. The power supply has a provision to increase the power with a step of 0.1 V. The Cu electrodes are connected to power supply with 10 gauge Cu wire and Cu lugs to have minimum resistance. Two pipes of $\frac{1}{4}$ inch diameter are used for circulation of cold water and hot water from the condenser, so that, the vapours form are converted to water and the volume of test cell remains unchanged. K-type thermocouple used for data logging. The data recorded by using RISHABH multi SI 232 data card. The shunt register (200A by 75 mV rating), connected in series with the test wire, that is used to measure the current through the wire.

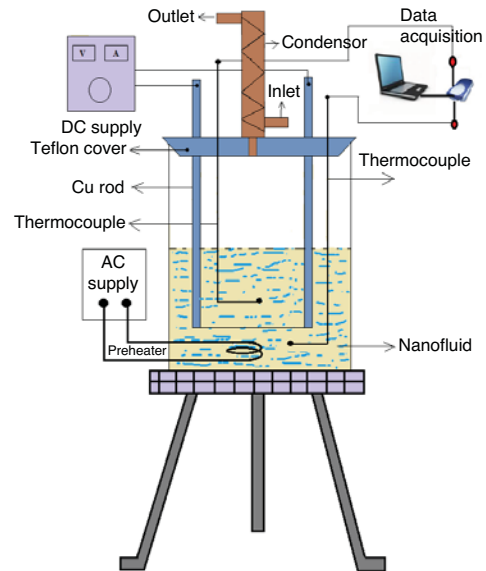


Figure 5: Schematic diagram of test rig

According to Asakura *et al.* [14], nanoparticles deposition on a surface during nucleate boiling is mainly influenced by heat flux of the heated surface, boiling time, concentration of nanoparticles and pH of the suspension.

Results and discussions

Pool boiling experiment is carried out using ZnO nanofluid and CHF is compared with DI water. Significantly improvement in CHF is observed. Figure 6 shows CHF values at different weight concentration of ZnO nanofluid.

The CHF of nanofluid has been compared with pure water by various researchers. The CHF enhancement is nearly 73% for stain steel wire with Al_2O_3 , ZrO_2 , and SiO_2 nanofluid, Kim *et al.* [15] the enhancement in CHF is only due to increase of contact area by deposition of nanoparticles over the heating surface. The nanoparticles generate porous layer on the test section tube surface thus reducing the contact angle between the fluid and heater surface. The existence of sorption layer enhance the trapping of liquid in nanoporous sorption layer and prevents the vapour blankets formation, so that the CHF increases with increasing the sorption layer thickness at lower particle concentration range.

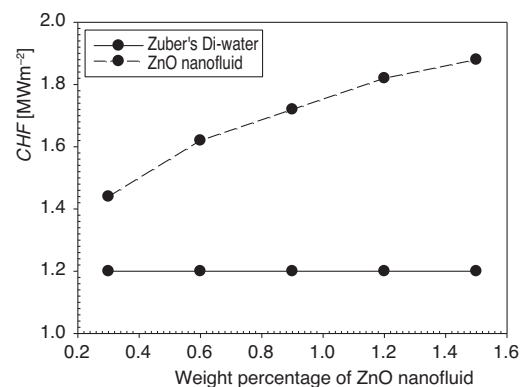


Figure 6. Variation in CHF with different weight concentration of ZnO nanofluid

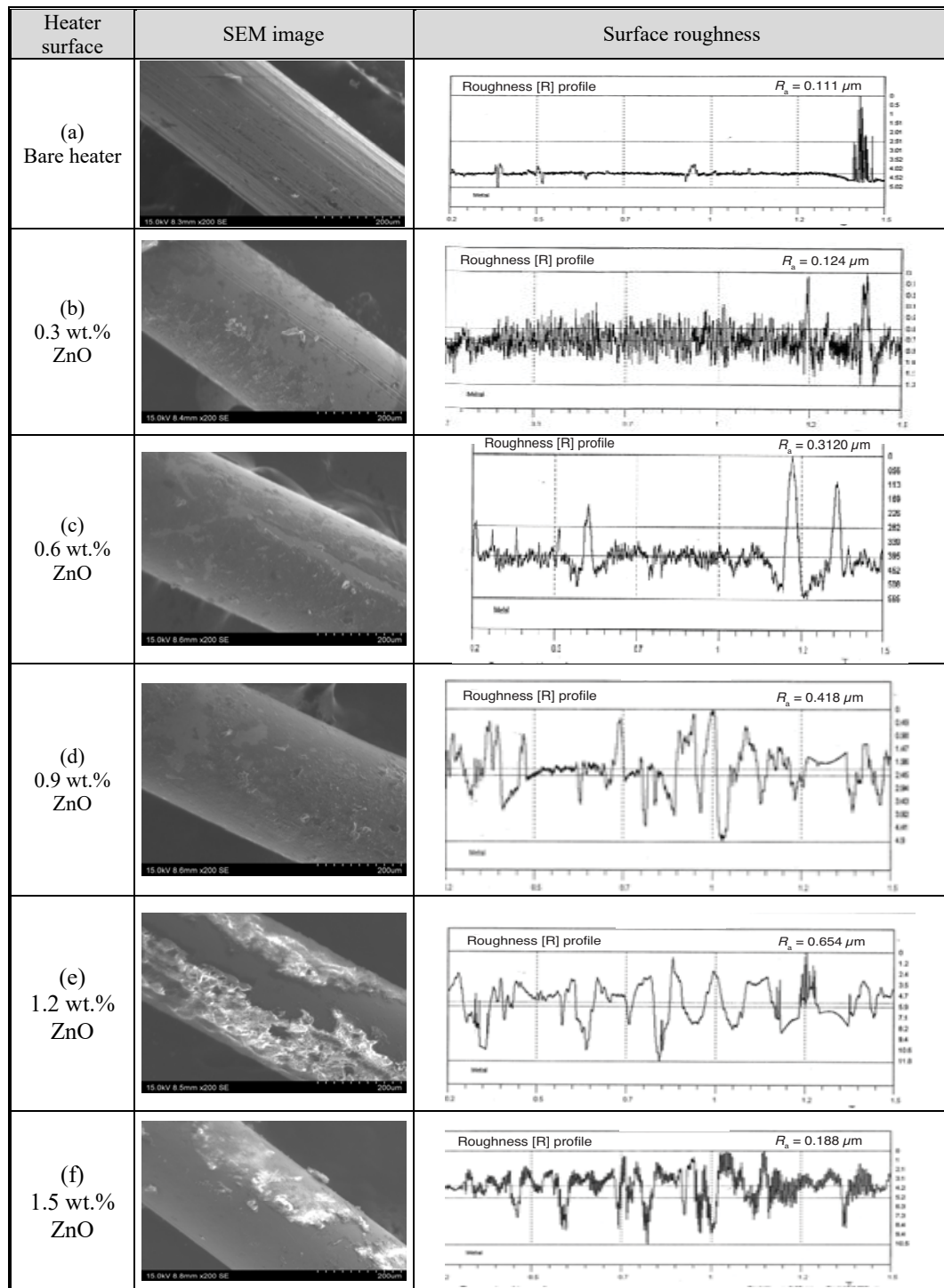


Figure 8. (a)-(f) The SEM image showing nanoparticles deposition on heater surface with different wt.% concentration of nanofluid and surface roughness of heater surface

Kshirsagar *et al.* [16] studied pool boiling with water based nanofluid and CuO nanoparticles. The results showed that the water-based nanofluid significantly enhanced CHF compared to that of pure water. The CHF values of the CuO nanofluid were enhanced from approximately 57.26% as compared to DI water. It was found that a sizable layer of nanoparticles deposits were formed on heater surface.

Ramakrishna *et al.* [17] investigate CHF enhancement using CuO nanofluid relative to CHF of pure water. The CHF values were measured for various volume concentrations, CHF enhancement 130% recorded for 0.2 volume percent of CuO.

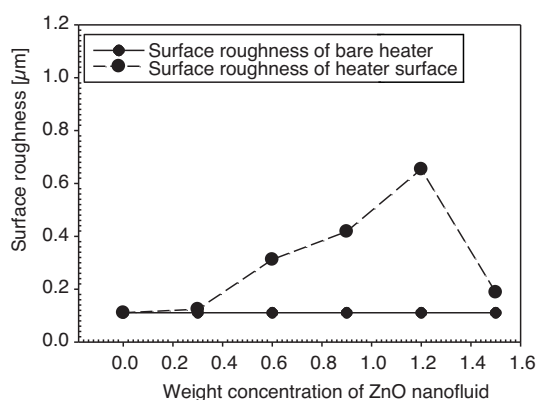


Figure 7. Increase in surface roughness with weight concentration of nanofluid

The results show that CHF enhancement is definitely possible by using different nanofluid instead of DI water for cooling fluids. However, the surface coating of heater surface is depending on particles concentrations of the nanofluid, a layer build up which may increase or decrease surface roughness that will depend upon porosity and nanoparticles size. The surface roughness measurement is taken when the test surface exposed to different weight concentration of nanofluid after pool boiling CHF tests made, known that CHF enhancement of nanofluid is closely related with the surface micro-structure and enhanced surroundings from the deposition of nanoparticles as shown in fig. 7.

The SEM image of heater surface are taken on which it is clearly observed that increase in surface roughness, SEM of bare heater also taken before starting the experiment. Bare heater roughness is measured is found to be 0.111 µm as shown in fig. 8 (a).

For all weight concentration of nanofluid SEM images are taken after conducting the experiment. The increase in roughness from 0.3 wt.% to 1.2 wt.% observed on the heater surface fig. 8(b)-8(e) and for 1.5 weight concentrations surface roughness suddenly decreases up to 0.188 µm.

The study of SEM image shows that deposition of nanoparticles on heater surface. So the porosity plays important role in boiling heat transfer even changes roughness and wettability.

Conclusions

In this study, pool boiling CHF behaviours on electrically heated Ni-Cr wire with nanoporous deposits were investigated at saturated temperature under atmospheric pressure. Various deposit structures were obtained by varying the increasing rate and maximum value of heat flux during the pre-boiling in different weight concentration of water-ZnO nanofluid.

Surface properties of the deposit wires were characterized to identify the major surface parameters associated with the significant CHF increases on a heater with nanoparticles deposits. It was found that heat capacity of heater surface in the present study changes due to the nanoparticles deposit so that it is not a major parameter in interpreting the increased CHF. Pool boiling characteristics in ZnO nanofluid were investigated with five weight concentrations 0.3, 0.6, 0.9, 1.2, and 1.5 wt.% of ZnO with DI water. The enhancement in CHF for every concentration is studied and the maximum enhancement of 47.16% CHF takes place at 1.5 wt.% of ZnO and for 0.3 wt.% is 13.88%.

During experimentation it is observed that roughness on heater surface increases up to 1.2 wt.% after that it suddenly decreases, even CHF increases slowly from 1.2. to 1.5 wt.%, rate of enhancement in CHF decreases from 1.2 to 1.5 wt.% of ZnO nanofluid.

The CHF enhancement is directly related with surface microstructure and enhanced topography resulting from the deposition of nanoparticles SEM image of the heater surface shows porous layer build up due to boiling induced precipitation of nanofluid. Decrease in surface roughness can be attributed to nanoparticles filling the microcavities formed over the heater surface.

Nomenclature

A – area of heater surface, [m²]
 D – diameter of heater, [m]
 h_{fg} – latent heat of vaporization, [kJkg⁻¹]
 I – current, [A]
 L – length of heater, [m]
 q – heat flux, [W]
 q_{CHF}^* – critical heat flux, [MWm⁻²]
 R_a – average roughness, [μm]
 T_s – temperature of heater surface, [°C]
 T_{sat} – saturation temperature, [°C]
 V – voltage, [V]

Greek symbols

β – full width half maxima of the peak, [radian]
 Δ – difference
 θ – peak, [radian]
 λ – X- ray wavelength of vapour jets, [m]
 ν – frequency, [Hz]

ρ – density, [kgm⁻³]
 ρ_l – density of liquid
 ρ_v – density of vapour
 σ – surface tension, [Nm⁻¹]

Subscripts

C – critical
fg – vaporization
HF – heat flux
l – liquid
sat – saturation
v – vapour

Acronyms

DI – deionises
CHF – critical heat flux
SEM – scanning electron microscopy
TEM – transmission electron microscopy

References

- [1] Kim, S., et al., Effects of Nano-Fluid and Surfaces with Nano Structure on the Increase of CHF, *Exp. Thermal Fluid Sci.*, 34 (2010), 4, pp. 487-495
- [2] Ozisik, M. N., *Heat Transfer, A basic Approach*, McGraw-Hill International Editions, N. Y., USA, 1985
- [3] Collier, J. G., Thome, J. R., *Convective Boiling and Convection*, 3rd ed., Oxford Science Publication, Oxford, UK. 2001
- [4] Piroo, I. L., et al., Nucleate Pool-Boiling Heat Transfer, I: Review of Parametric Affects of Boiling Surface, *Int. J. Heat Mass Transfer*, 47 (2004), 23, 5033-5044
- [5] Piroo, I. L., et al., Nucleate Pool-Boiling Heat Transfer, II: Review Assessment of Prediction Methods, *Int. J. Heat Mass Transfer*, 47 (2004), 23, 5045-5057
- [6] Jagdeep, M., et al., Review of the Influence of Nanoparticles on Thermal Conductivity, Nucleate Pool Boiling and Critical Heat Flux, *Heat Mass Transfer*, 51 (2015), 3, pp. 381-398
- [7] Kim, M., et al., Experimental Study on CHF Characteristics of Water-TiO₂ Nanofluid, *Nucl. Eng. Technol.*, 38 (2006), 1, pp. 61-69
- [8] Pitts, C. C., Leppert, G., The Critical Heat Flux for Electrically Heated Wires in Saturated Pool Boiling, *Int. J. Heat Mass Transfer*, 9 (1966), 4, pp. 365-370, IN363–IN364, pp. 371-377
- [9] Van Stralen, S. J. D., Sluyter, W. M., Investigations on the Critical Heat Flux of Pure Liquids and Mixtures under Various Conditions, *Int. J. Heat. Mass Transfer*, 12 (1969), 11, pp. 1353-1384
- [10] Sun, K.-H., Lienhard, J. H., The Peak Pool Boiling Heat Flux on Horizontal Cylinders, *Int. J. Heat Mass Transfer*, 13 (1970), 9, pp. 1425-1430, IN1421–IN1423, pp. 1431-1439
- [11] Bakhru, N., Lienhard, J. H., Boiling from Small Cylinders, *Int. J. Heat Mass Transfer*, 15 (1972), 11, pp. 2011-2025
- [12] You, S. M., et al., The Onset of Film Boiling on Small Cylinders: Local Dry Out and Hydrodynamic Critical Heat Flux Mechanisms, *Int. J. Heat. Mass Transfer*, 37 (1994), 16, pp. 2561-2569
- [13] Holman, J. P., *Experimental Methods for Engineer's*, 7th ed., Chap. 3, McGraw-Hill, N. Y., USA, (2007)

- [14] Asakura, Y., *et al.*, Deposition of Iron Oxide on Heated Surfaces in Boiling Water, *Nucl. Sci. Eng.*, 67 (1978), 1, pp. 1-7
- [15] Kim, S. J., *et al.*, Surface Wettability Changes during Pool Boiling of Nanofluids and its Effect on Critical Heat Flux, *Int. Journal of Heat Mass Transfer*, 50 (2007), 19-20, pp. 4105-4116
- [16] Jagdeep, M., *et al.*, Preparation and Characterization of Copper Oxide Nanoparticles and Determination of Enhancement in Critical Heat Flux, *Thermal Science*, 21 (2017), 1A, pp. 233-242
- [17] Ramkrishna, N., Hegde, S., Rao, S., Reddy, R. P., Investigation on Heat Transfer Enhancement in Pool Boiling with Water-CuO Nanofluids, *Journal of Thermal Science*, 21 (2012), 2, pp. 179-183